Microchimica Acta (2020) 187: 679
https://doi.org/10.1007/s00604-020-04657-1

ORIGINAL PAPER

Immunoassay for foodborne pathogenic bacteria using magnetic composites Ab@Fe_3O_4, signal composites Ap@PtNp, and thermometer readings

Shengjun Bu[1] · Kuiyu Wang[2] · Chengyu Wang[1] · Zhongyi Li[1] · Zhuo Hao[1] · Wensen Liu[1] · Jiayu Wan[1]

Received: 10 August 2020 / Accepted: 18 November 2020 / Published online: 28 November 2020

Abstract

A point-of-care (POC) immunoassay was established for the sensitive and rapid detection of pathogenic *Escherichia coli* O157:H7, using magnetic Fe_3O_4 organic-inorganic composites (Ab@Fe_3O_4) for immunomagnetic separation, nanozyme platinum nanoparticle (PtNp) organic-inorganic composites (Ap@PtNp) for signal amplification, and thermometer readings. Antibodies and Fe_3O_4 were incubated in Cu^{2+} phosphate buffer to synthesize the magnetic composite Ab@Fe_3O_4 with antibodies, to specifically capture *E. coli* O157:H7. Antimicrobial peptides and PtNp were incubated in Cu^{2+} phosphate buffer to synthesize the signal composites Ap@PtNp with antimicrobial peptides (magainin I), recognizing and labeling *E. coli* O157:H7. In the presence of *E. coli* O157:H7, magnetic microcomposites targeted bacteria and signal microcomposites to form the sandwich structure: Ab@Fe_3O_4-bacteria-Ap@PtNp for magnetic separation. Ap@PtNp of signal composites catalyzed H_2O_2 to generate thermo-signals (temperature rise), which were determined by a thermometer. This point-of-care bioassay detected *E. coli* O157:H7 in the linear range of 10^1–10^7 CFU mL^{-1} and with a detection limit of 14 CFU mL^{-1}.

Keywords Foodborne pathogenic bacteria · Point of care · Organic-inorganic composites · Thermal signal

Introduction

Foodborne diseases caused by pathogenic bacteria have become a global public health problem, posing a significant threat to human health [1]. It is widely recognized that the rapid, sensitive, and specific detection of pathogens is becoming more important in controlling illness outbreaks [2]. However, access to laboratory tests remains limited in some poor countries, and also in some developing countries [3]. The rapid, sensitive, and specific point-of-care (POC) detection of foodborne pathogenic bacteria can effectively reduce food- and water-borne outbreaks, especially in resource-limited settings [4]. Other common methods of detecting pathogenic bacteria use microbiological plating and counting and the polymerase chain reaction (PCR). Although these approaches are specific and sensitive, their applications in such settings are limited as they are easy to contaminate and generate false-positive results [5].

Over recent decades, scientists have successfully developed viable POC bioassays, based on immunoassay to detect foodborne pathogenic bacteria [6]. POC testing has the advantage of greater availability in resource-constrained areas when compared to standard laboratory-based diagnostics. Currently, the main challenge of the POC bioassay is the detection of pathogenic bacteria in food, and the amplification and conversion of associated signals into readable digital outputs on portable devices.

Magnetic nanoparticles (MNPs) have been widely used for the capture and enrichment of pathogenic bacteria in complex food samples [7]. MNPs have unique properties: (1) they are easily manipulated by magnets; (2) they contain rapid solution kinetics and high surface volume ratios to ensure magnetic separation of targets (e.g., pathogenic bacteria); and (3) they have reduced matrix effects [8, 9]. MNPs are excellent candidates for POC immune assays, as they can be developed into

✉ Wensen Liu
Liuws85952@163.com

✉ Jiayu Wan
wanjiayu@hotmail.com

[1] Institute of Military Veterinary, Academy of Military Medical Sciences, Changchun 130122, China

[2] School of Chemical Engineering and Technology, Sun Yat-sen University, Zhuhai 519082, China

multifunctional bioassay materials, with great potential [10]. To label and enrich for target bacteria, MNPs require biomolecular modifications that recognize targets using complex reagents such as antibodies, aptamers, peptides, carbohydrates, and antibiotics [11]. In recent years, a facile approach for preparing organic-inorganic microcomposites with flower-like construction has been reported; it uses phosphate as an inorganic component and protein as an organic component [12]. Due to its high surface volume ratio, facile synthesis, and outstanding protein compatibility, these organic-inorganic microcomposites have attracted great attention [13]. When compared with traditional protein affixation methods, microcomposites can effectively maintain and even improve protein activity [14]. Spurred on by this facile approach, our research group observed that some nanoparticles (e.g., hemin and MnO_2) could be embedded into organic-inorganic microcomposites, which are capable of biological recognition and signal amplification for the POC detection of foodborne pathogenic bacteria [15, 16]. In this study, the magnetic nanoparticles Fe_3O_4 and pathogenic bacterial antibodies were incubated in Cu^{2+} phosphate buffer to synthesize magnetic organic-inorganic microcomposites for the enrichment and immune-separation of foodborne pathogenic bacteria. To the best of our knowledge, antibody-$Cu_3(PO_4)_2$ microcomposites loading Fe_3O_4 nanoparticles (magnetic microcomposites, MMC) have not been reported for the magnetic separation of pathogenic bacteria.

Transducers perform a vital role in the specificity and the signal detection of POC bioassays [17]. Bio-recognition signals from pathogenic bacteria are transformed into quantifiable signals using such transducers [18]. Recently, scientists have developed a variety of transduction methods, applied to the detection of foodborne pathogenic bacteria [19]. Signal transduction modes and physical parameters, such as electrochemical, optical, mass, and pH, are used for signal analysis in bioassays. The development of temperature-sensing technologies has an important practical significance across many fields, such as meteorology, chemistry, pharmacy, biology, and the military [20, 21]. It is encouraging that the emergence of thermo-based bioassays has opened up a new field of biosensing systems [22]. Thermometers, as an inexpensive, easy-to-use, fast, and real-time reading independent instrument, provide a powerful, portable, reliable, fast, and cheap detection tool for clinical biomarkers and other analyses [23].

Due to its catalytic efficiencies, excellent stability in harsh environments, ease of production, high efficiencies, and affinity for substrates, nanozyme platinum nanoparticles (PtNp) have been used as substitutes for natural enzymes in immunoassay signal amplification [24]. Our previous research found that PtNp catalyzed the decomposition of H_2O_2 into O_2, which caused a significant increase in temperature across the reaction system [25]. PtNp can transform target biological identification processes into quantifiable temperature signals. However, PtNp must be coupled to target biomolecules via a complex process. In this study, the nanozyme, PtNp, and magainin I were incubated in Cu^{2+} phosphate buffer to synthesize a nanozyme Ap@PtNp (signal microcomposites, SMC) as a signal-transforming label for foodborne pathogenic bacteria.

We developed a rapid and portable bioassay for detecting foodborne pathogenic bacteria by used *Escherichia coli* O157:H7 as a model pathogen (Scheme 1). This immunoassay combined magnetic separation using magnetic microcomposites, Ab@Fe_3O_4, and signal amplification using signal microcomposites Ap@PtNp, with thermo-signal analysis, using a thermometer. In the presence of the target *E. coli* O157:H7, a sandwich structure Ab@Fe_3O_4-bacteria-Ap@PtNp was formed (Scheme 1). H_2O_2 decomposition was catalyzed by the nanozyme platinum of SMC to produce thermo. Finally, a thermometer was used to detect temperature changes for the quantitative determination of the target pathogen, *E. coli* O157:H7.

Materials and methods

Reagents and setup

Phosphate-buffered saline (PBS, 0.01 M) (0.01 M NaH_2PO_4 and 0.01 M Na_2HPO_4, pH 7.4) were procured from Invitrogen, Germany (https://www.thermofisher.com/us/en/home.html). Ferro ferric oxide (Fe_3O_4), copper sulfate pentahydrate ($CuSO_4 \cdot 5H_2O$), and the magainin I (GIGKFLHSAGKFGKAFVGEIMKS) peptide were obtained from Sangon Biotech (Shanghai, China, www.sangon.com). PtNp (10 nm) were obtained from Beijing Dk Nanotechnology Co., Ltd. (Beijing, China), and H_2O_2 (30 wt%) was purchased from Shanghai Ling Feng Chemical Regent Co., Ltd. (Shanghai, China, http://lfhxsj.cn.b2b168.com/). *E. coli* O157:H7 antibodies were supplied by Abcam (ab252713, Shanghai, China, www.abcam.cn). All other chemicals were from Sinopharm Chemical Reagent Beijing Co., Ltd. (Beijing, China, http://www.crc-bj.com/) and were analytical grade. Deionized water was used in all experimental procedures and was ultra-filtered using a Millipore Milli-XQ system (18.3 MΩ cm, Billerica, MA, USA, www.merckmillipore.com). Bacterial strains of *Salmonella typhimurium*, (Sal, CICC 21484), *Staphylococcus aureus* (Sta, CICC 10384), *Listeria monocytogenes* (Lis, CICC 21635), and *Escherichia coli* O157:H7 (*E. coli* O157:H7, CICC 24187) were purchased from China Center of Industrial Culture Collection (Beijing, China, http://www.china-cicc.org). A digital thermometer (model number SJPT302), with a temperature detection range of − 50 to + 300 °C (degree precision = 0.1 °C) was obtained from Sensegene flagship store (Hangzhou, China, http://www.sensegene.com/).

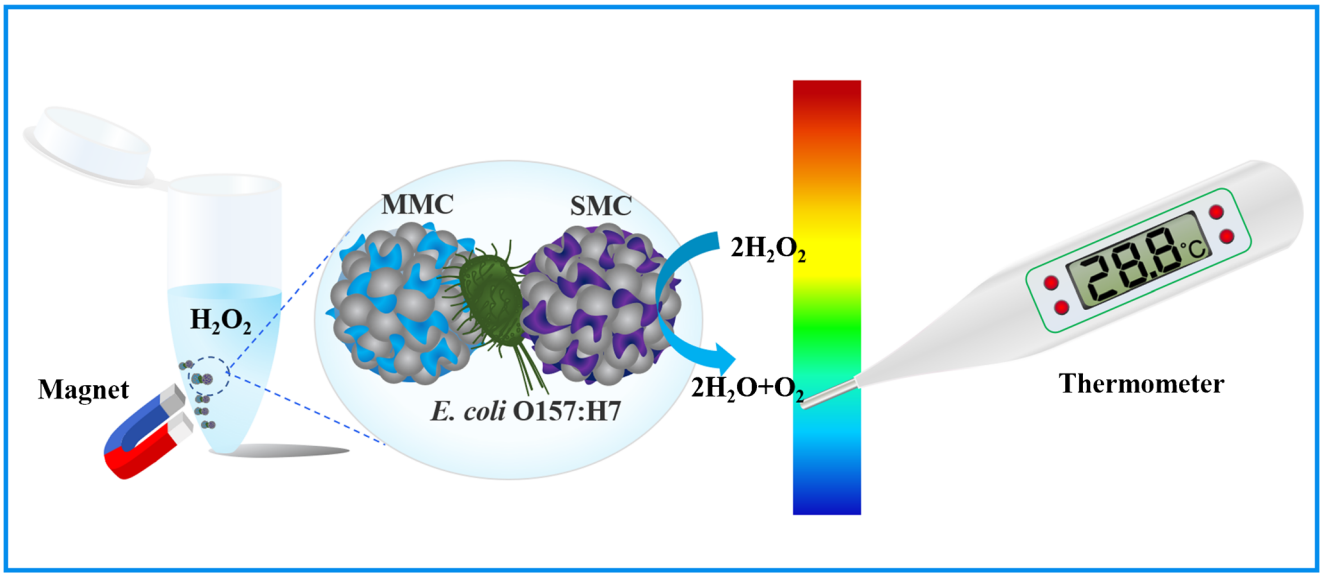

Scheme 1 Schematic diagram of the exothermic immunosensor system based on MMC and SMC for the determination of *E. coli* O157:H7 (magnetic microcomposites Ab@Fe_3O_4, MNC; signal microcomposites Ap@PtNp, SMC)

Scanning electron microscopy (SEM) images were obtained using a JEOL JEM-2100 (Tokyo, Japan, https://www.jeol.co.jp/). X-ray diffraction (XRD) measurements were determined using an X-ray polycrystal diffractometer (Beijing Purking General Instrument Co., Ltd. XD6, Beijing, China, www.pgeneral.com.cn).

Preparation of Ab@Fe_3O_4 and Ap@PtNp microcomposites

Ab@Fe_3O_4 and Ap@PtNp were prepared according to a previously published report, with a slight modification [26]. Details are also specified in the Supporting Material. The capture efficiency of Ab@Fe_3O_4 was measured by conventional plate method. The capture efficiency (%) = $X/Y \times 100\%$, where X are *E. coli* O157:H7 numbers after magnetic capture, and Y are *E. coli* O157:H7 numbers before magnetic separation.

The detection of *E. coli* O157:H7 using a thermometer

Firstly, 100 μL of different *E. coli* O157:H7 densities (10^1, 10^2, 10^3, 10^4, 10^5, 10^6, 10^7, 10^8 CFU mL^{-1}) were added to a 5-μL Ab@Fe_3O_4 solution, followed by the addition of 10-μL Ap@PtNp microcomposite, to a final volume of 115 μL. The mixture was incubated for 90 min at 35 °C. The reaction mixture was then washed four times in PBS (0.1 mM, pH 7), using a magnetic separation rack to remove unbound microcomposites. Finally, 600-μL H_2O_2 (30 wt%) was added to generate a decomposition reaction, producing heat. After 7 min, the final reaction temperature was measured. As shown (Fig. S1), the thermosignal was considerably increased before (left image) and after H_2O_2 decomposition (right image). The temperature was obtained from this mixture. The major advantage of this assay is the omission of traditional sandwich cleaning steps; a one-step cleaning method is required. When compared with other sandwich methods, our approach had a simpler cleaning procedure and reduced incubation times (Table 1).

Real food assay to determine target *E. coli* O157:H7

The standard addition method was used to calculate recovery [33]. Briefly, 10^3, 10^4, and 10^5 CFU mL^{-1} *E. coli* O157:H7 densities were diluted in PBS (0.1 mM, pH 7). After this, bacteria were added to 1-mL commercial milk, and detected under optimized experimental conditions. Using our linear calibration curves and thermo-signals, target *E. coli* O157:H7 densities were determined from six independent experiments.

Data analysis

The temperature change (ΔT) was represented as the difference between the thermal signals measured by the digital thermometer in the presence and absence of the target bacteria. The experiment date were performed at least three independent experiments (mean ± standard deviation (SD)) and analyzed by GraphPad PRIME (7.0) software.

Results and discussion

Characterization of Ab@Fe_3O_4 and Ap@PtNp

We report a novel approach that directly synthesizes Ab@Fe_3O_4 that exhibits magnetic properties and hierarchical structures. The morphology of microcomposite of ferrites were characterized by SEM. As shown (Fig. 1a and b), typical

Table 1 Comparison of different sandwich techniques for pathogenic bacteria detection

Target	Cleaning frequency (times)	Incubation time (hour)	Reference
Salmonella enteritidis	6	14	[27]
Salmonella typhimurium	4	2	[28]
Salmonella typhimurium	5	1.8	[29]
Salmonella typhimurium	6	24.5	[30]
Staphylococcus aureus	8	3.4	[31]
E. coli O157:H7	6	2.4	[32]
E. coli O157:H7	4	1.5	Our work

SEM images show a spherical structure, with a coarse surface and an average spherical diameter of approximately 12 μm. These dimensions and characteristics illustrate that Ab@Fe_3O_4 morphology was similar to previous hybrid nanoflowers [26]. This was in accordance with our SEM characterization results. These microcomposites not only immobilized Fe_3O_4, but their high ratio to surface areas, and their good space utilization ratios for efficient antibody entrapment effectively captured the target. In addition, the larger specific surface areas of Ab@Fe_3O_4 microcomposites also facilitated the application of related surface reactions. They also provided intrinsic magnetism, allowing the target molecule to be quickly separated from the complex mixture, by a magnetic field in a short time. Similarly, Ap@PtNp had the properties of the catalytic activity of platinum that could be used for the dissociation of H_2O_2 molecules. This catalytic process produced heat which was processed as a final signal output. As shown (Fig. 1c and d), SEM images of Ap@PtNp

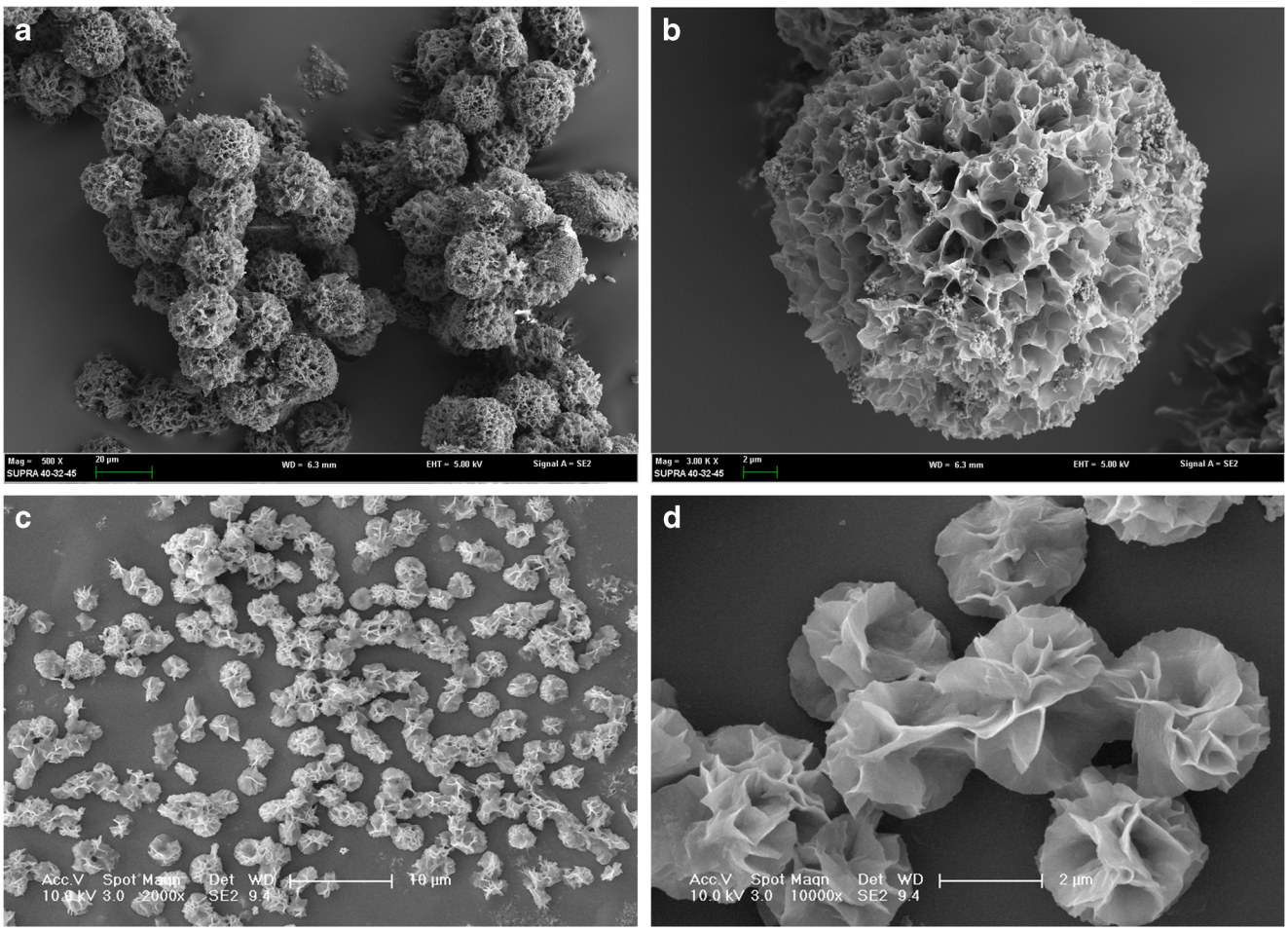

Fig. 1 Characterization of microcomposites. SEM images of (**a**) Ab@Fe_3O_4 (scale; 20 μm), (**b**) Ab@Fe_3O_4 (scale; 2 μm), (**c**) Ap@PtNp (scale; 10 μm), and (**d**) Ap@PtNp (scale; 2 μm)

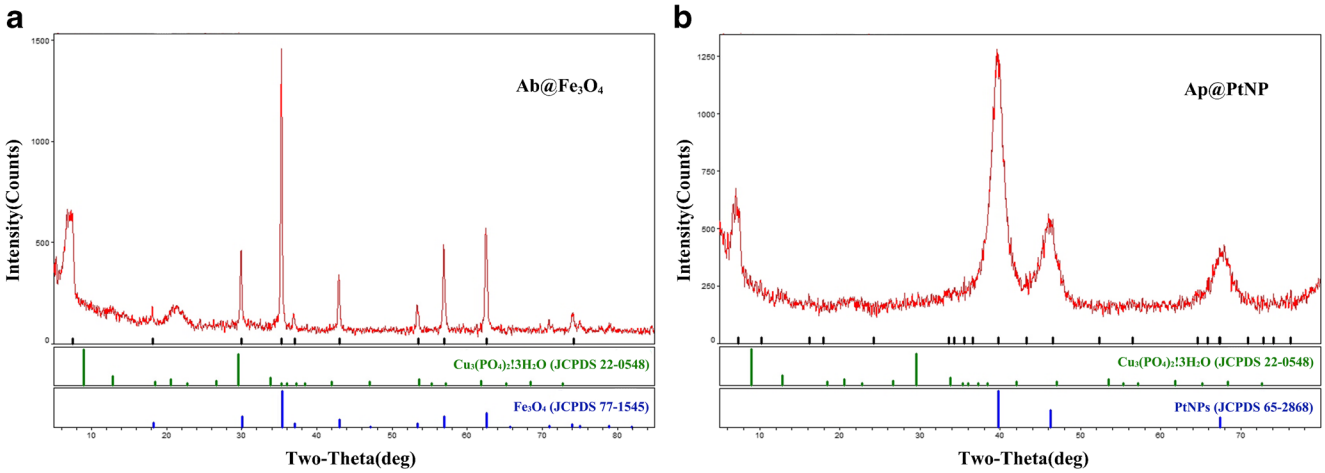

Fig. 2 XRD characterization patterns of (**a**) Ab@Fe_3O_4 (red line) and $Cu_3(PO_4)_2{\cdot}3H_2O$ (green line) and Fe_3O_4 (blue line) (**b**) Ap@PtNp (red line), $Cu_3(PO_4)_2{\cdot}3H_2O$ (green line), and PtNP (blue line)

displayed a classic form, similar to the morphology of Ab@Fe_3O_4, with an average diameter of approximately 3 μm.

The crystal structure and crystallinity of Ab@Fe_3O_4 and Ap@PtNp were recorded by XRD in the range at 2θ = 5° − 85° on a desktop X-ray diffractometer. Figure 2 a indicates the Ab@Fe_3O_4 fitted well with $Cu_3(PO_4)_2{\cdot}3H_2O$ (JCPDS file 22-0548) and Fe_3O_4 (JCPDS file 77-1545), revealing the copper phosphate and ferro ferric oxide in the nanoparticles. These characteristic signals appeared for Ab@Fe_3O_4, suggesting that the synthesis of Ab@Fe_3O_4 was crystalline. Similarly, XRD pattern for Ap@PtNp (Fig. 2b) confirmed that microcomposites consisted of crystalline nanoparticles ($Cu_3(PO_4)_2{\cdot}3H_2O$ (JCPDS file 22-0548 and PtNP JCPDS file 65-2868). In addition, Ab@Fe_3O_4 and Ap@PtNp microcomposite stability was investigated to confirm that the antibody and magainin I still maintained initial activities. As shown (Fig. S2), no thermo-signal changes were observed for *E. coli* O157: H7 detection up to 60 days at 4 °C, thus confirming microcomposite stability up to 2 months. These results suggested that microcomposites had been successfully generated for further studies.

Optimization conditions

Several different parameters were optimized: Fig. S3 A; antibody immobilization on Ab@Fe_3O_4, i.e., 8 μg mL^{-1}; (B) Fe_3O_4 particles in Ab@Fe_3O_4, 1.2 mg mL^{-1}; Fig. S4; the effects of Ab@Fe_3O_4 volume composites on capture efficiency, 5 μL; Fig. S5; (A) the concentration of magainin I, 15 μg mL^{-1}; (B) the concentration of PtNp in Ap@PtNp, 0.5 μg mL^{-1}; Fig. S6; (A) reaction temperature, 35 °C; (B) reaction time, 90 min, and (C) pH 7.

Quantitative detection of *E. coli* O157: H7

Under optimized reaction conditions, *E. coli* O157: H7, at different cell densities, was added to immunoassays to ascertain detection sensitivities. As shown (Fig. 3), a linear relationship was observed between the thermo-signal and the *E. coli* O157: H7 cell density logarithmic scale, in the range 10^1–10^7 CFU mL^{-1}. A correlation coefficient of 0.975 (Fig. 3b) was also recorded. The linear equation was $Y = 1.631*X + 0.1$. We also determined the limit of detection (LOD) using the

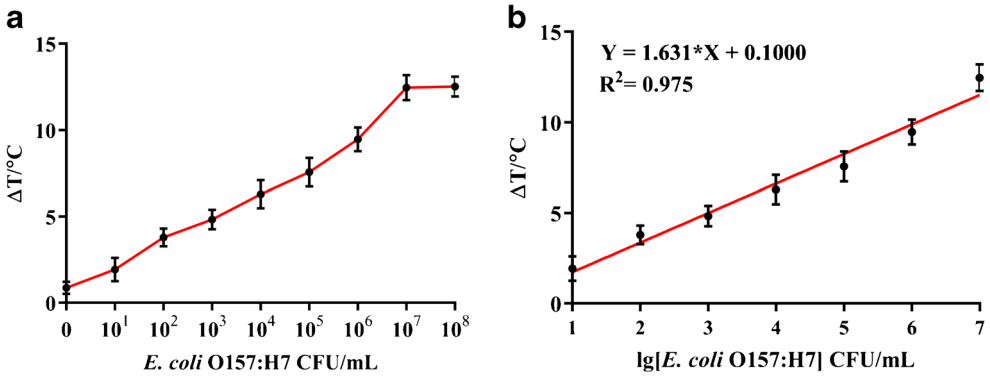

Fig. 3 Relationship between ΔT and different target concentrations. **a** 0–10^8 CFU mL^{-1} *E. coli* O157:H7 and **b** linear relationship between ΔT and logarithmic *E. coli* O157:H7 concentrations, 10–10^7 CFU mL^{-1}. Three independent experiments were conducted

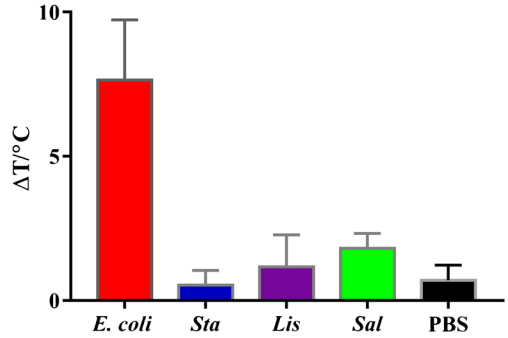

Fig. 4 System selectivity. Target bacteria, *E. coli* O157:H7, and other bacteria (*Staphylococcus aureus* (*Sta*); *Listeria monocytogenes* (*Lis*); and *Salmonella typhimurium* (*Sal*)) were used at a cell density of 10^7 CFU mL^{-1}. PBS was used as a control at 0.1 mM (pH = 7). All experimental conditions were optimized and three independent experiments were conducted

following formula: 3σ/slope [34] (where σ is the standard deviation of blank samples). The LOD was 14 CFU mL^{-1}, which was superior or comparable to other immunoassay detection limits (Table S1). These materials were easy to bioassay and prepare without any particular molecular interactions that supplies the results compare to other antibody/magainin I-based detection method of pathogenic bacteria [35]. The synthetic processing of this material efficiently eliminated the damage of recognizing element (antibody or magainin I) during immobilization. The main advantage of Ab@Fe_3O_4 and Ap@PtNp materials was that they integrated recognition, separation, and signal release functions to achieve a one-step cleaning detection. Hence, our bioassay had a simpler synthetic procedure and operation steps, when compared with other materials (e.g., metal-organic framework [36]), or common pathogen detection methods (e.g., ELISA [37]). Such sensitive sensing performances may be ascribed to the following: (a) magnetic microcomposites containing millions of Fe_3O_4 particles and target antibody sites, thus achieving significant target accumulation and magnetic separation, allowing thermal signal responses to be efficiently amplified; (b) signal microcomposites also have millions of material binding sites which can be layer-by-layer deposited by PtNp and peptides. Thus, the dual-microcomposite immunoassay structure exhibited great specificity for the sensitive detection of *E. coli* O157: H7.

Bioassay selectivity and reproducibility

To further confirm assay selectivity, several common foodborne pathogens were assessed; *E. coli* O157:H7, *Sal*, *Lis*, *Sta*, and a control (PBS) were investigated. Our data demonstrated that Ab@Fe_3O_4 and Ap@PtNp selectively captured only *E. coli* O157:H7 (Fig. 4). Equally, *E. coli* O157:H7 at densities of 10^2 CFU mL^{-1}, 10^3 CFU mL^{-1}, and 10^4 CFU·mL^{-1} were used to identify bioassay coefficients of variation (CV). Our data indicated that CV of 2.37%, 2.04%, and 2.24%, respectively, were achieved (in quintuplicate), thereby indicating bioassay reproducibility towards target *E. coli* O157:H7 detection.

Detection of *E. coli* O157: H7 in spiked milk samples

To truly evaluate system long-term stability in complex samples, the system was evaluated to detect different *E. coli* O157:H7 cell densities spiked into sterile pure milk. Thermo-signals were obtained and the results summarized (Table S2). These data showed that recoveries of 97.2–115.3% were achieved for milk samples by standard addition methods, with a relative standard deviation (RSD) of 3.9–10.8% ($n = 6$). This method showed an acceptable reproducibility, and has the potential to be used for complex biological samples. These results also demonstrated that the immunoassay possessed improved detection capabilities for pathogenic bacteria, with high sensitivity and accuracy.

Conclusions

In this study, a sensitive, rapid, and portable bioassay was successfully developed for detecting *E. coli* O157:H7 in complex food samples. The system was based on Ab@Fe_3O_4 microcomposite immunomagnetic separation, Ap@PtNp microcomposite signal amplification, and thermometer readings. Utilization of these materials of Ab@Fe_3O_4 and Ap@PtNp efficient guarantee this method's sensitivity and selectivity. These microcomposites need to be simplified the synthetic steps when it is be appropriate for non-professionals. Nevertheless, this POC bioassay has great potential for screening in-field foodborne pathogenic bacteria.

Supplementary Information The online version contains supplementary material available at https://doi.org/10.1007/s00604-020-04657-1.

Funding This work was financially supported by the National Key Research and Development Program of China (no. 2016YFD0501001).

Compliance with ethical standards

Conflict of interest The authors declare they have no competing interests.

References

1. Chlebicz A, Slizewska K (2018) Campylobacteriosis, salmonellosis, yersiniosis, and listeriosis as zoonotic foodborne diseases: a review. Int J Env Res Public Health 15 (5). doi: ARTN 863 https://doi.org/10.3390/ijerph15050863
2. Kant K, Shahbazi MA, Dave VP, Ngo TA, Chidambara VA, Than LQ, Bang DD, Wolff A (2018) Microfluidic devices for sample preparation and rapid detection of foodborne pathogens.

Biotechnol Adv 36(4):1003–1024. https://doi.org/10.1016/j.biotechadv.2018.03.002
3. Xianyu YL, Wang QL, Chen YP (2018) Magnetic particles-enabled biosensors for point-of-care testing. Trac-Trends in Analytical Chemistry 106:213–224. https://doi.org/10.1016/j.trac.2018.07.010
4. Chen J, Andler SM, Goddard JM, Nugen SR, Rotello VM (2017) Integrating recognition elements with nanomaterials for bacteria sensing. Chem Soc Rev 46(5):1272–1283. https://doi.org/10.1039/c6cs00313c
5. Wu Z, Fu Q, Yu S, Sheng L, Xu M, Yao C, Xiao W, Li X, Tang Y (2016) Pt@AuNPs integrated quantitative capillary-based biosensors for point-of-care testing application. Biosens Bioelectron 85:657–663. https://doi.org/10.1016/j.bios.2016.05.074
6. Rubab M, Shahbaz HM, Olaimat AN, Oh DH (2018) Biosensors for rapid and sensitive detection of Staphylococcus aureus in food. Biosens Bioelectron 105:49–57. https://doi.org/10.1016/j.bios.2018.01.023
7. El-Boubbou K, Gruden C, Huang X (2007) Magnetic glyco-nanoparticles: a unique tool for rapid pathogen detection, decontamination, and strain differentiation. J Am Chem Soc 129(44):13392–13393. https://doi.org/10.1021/ja076086e
8. Xianyu Y, Chen Y, Jiang X (2015) Horseradish peroxidase-mediated, iodide-catalyzed cascade reaction for plasmonic immunoassays. Anal Chem 87(21):10688–10692. https://doi.org/10.1021/acs.analchem.5b03522
9. Chen YP, Xianyu YL, Wu J, Yin BF, Jiang XY (2016) Click chemistry-mediated nanosensors for biochemical assays. Theranostics 6(7):969–985. https://doi.org/10.7150/thno.14856
10. Fu S, Wang S, Zhang X, Qi A, Liu Z, Yu X, Chen C, Li L (2017) Structural effect of Fe3O4 nanoparticles on peroxidase-like activity for cancer therapy. Colloids Surf B Biointerfaces 154:239–245. https://doi.org/10.1016/j.colsurfb.2017.03.038
11. Zhu MJ, Liu WP, Liu HX, Liao YH, Wei JT, Zhou XM, Xing D (2015) Construction of Fe3O4/vancomycin/PEG magnetic nanocarrier for highly efficient pathogen enrichment and gene sensing. ACS Appl Mater Interfaces 7(23):12873–12881. https://doi.org/10.1021/acsami.5b02374
12. Ye R, Zhu C, Song Y, Song J, Fu S, Lu Q, Yang X, Zhu MJ, Du D, Li H, Lin Y (2016) One-pot bioinspired synthesis of all-inclusive protein-protein nanoflowers for point-of-care bioassay: detection of E. coli O157:H7 from milk. Nanoscale 8(45):18980–18986. https://doi.org/10.1039/c6nr06870g
13. Cui J, Jia S (2017) Organic–inorganic hybrid nanoflowers: a novel host platform for immobilizing biomolecules. Coord Chem Rev 352:249–263. https://doi.org/10.1016/j.ccr.2017.09.008
14. Guo RY, Wang SY, Huang FC, Chen Q, Li YB, Liao M, Lin JH (2019) Rapid detection of Salmonella Typhimurium using magnetic nanoparticle immunoseparation, nanocluster signal amplification and smartphone image analysis. Sensors and Actuators B-Chemical 284:134–139. https://doi.org/10.1016/j.snb.2018.12.110
15. Bu S, Wang K, Ju C, Wang C, Li Z, Hao Z, Shen M, Wan J (2019) Point-of-care assay to detect foodborne pathogenic bacteria using a low-cost disposable medical infusion extension line as readout and MnO2 nanoflowers. Food Control 98:399–404. https://doi.org/10.1016/j.foodcont.2018.11.053
16. Wang KY, Bu SJ, Ju CJ, Li CT, Li ZY, Han Y, Ma CY, Wang CY, Hao Z, Liu WS, Wan JY (2018) Hemin-incorporated nanoflowers as enzyme mimics for colorimetric detection of foodborne pathogenic bacteria. Bioorg Med Chem Lett 28(23–24):3802–3807. https://doi.org/10.1016/j.bmcl.2018.07.017
17. Fu MH, Xing JF, Ge ZQ (2019) Preparation of laccase-loaded magnetic nanoflowers and their recycling for efficient degradation of bisphenol a. Sci Total Environ 651:2857–2865. https://doi.org/10.1016/j.scitotenv.2018.10.145
18. Ye R, Zhu C, Song Y, Lu Q, Ge X, Yang X, Zhu MJ, Du D, Li H, Lin Y (2016) Bioinspired synthesis of all-in-one organic-inorganic hybrid nanoflowers combined with a handheld pH meter for on-site detection of food pathogen. Small 12(23):3094–3100. https://doi.org/10.1002/smll.201600273
19. Yang H, Li H, Jiang X (2008) Detection of foodborne pathogens using bioconjugated nanomaterials. Microfluid Nanofluid 5(5):571–583. https://doi.org/10.1007/s10404-008-0302-8
20. Zhang JJ, Xing H, Lu Y (2018) Translating molecular detections into a simple temperature test using a target-responsive smart thermometer. Chem Sci 9(16):3906–3910. https://doi.org/10.1039/c7sc05325h
21. Fu G, Sanjay ST, Zhou W, Brekken RA, Kirken RA, Li X (2018) Exploration of nanoparticle-mediated photothermal effect of TMB-H2O2 colorimetric system and its application in a visual quantitative photothermal immunoassay. Anal Chem 90(9):5930–5937. https://doi.org/10.1021/acs.analchem.8b00842
22. Qin TY, Liu B, Zhu KN, Luo ZJ, Huang YY, Pan CJ, Wang L (2018) Organic fluorescent thermometers: highlights from 2013 to 2017. Trac-Trends in Analytical Chemistry 102:259–271. https://doi.org/10.1016/j.trac.2018.03.003
23. Zhu JL, Wen MQ, Wen W, Du D, Zhang XH, Wang S, Lin YH (2018) Recent progress in biosensors based on organic-inorganic hybrid nanoflowers. Biosens Bioelectron 120:175–187. https://doi.org/10.1016/j.bios.2018.08.058
24. Zhu Z, Guan ZC, Liu D, Jia SS, Li JX, Lei ZC, Lin SC, Ji TH, Tian ZQ, Yang CYJ (2015) Translating molecular recognition into a pressure signal to enable rapid, sensitive, and portable biomedical analysis. Angewandte Chemie-International Edition 54(36):10448–10453. https://doi.org/10.1002/anie.201503963
25. Wang KY, Bu SJ, Ju CJ, Han Y, Ma CY, Liu WS, Li ZY, Li CT, Wan JY (2019) Disposable syringe-based visual immunotest for pathogenic bacteria based on the catalase mimicking activity of platinum nanoparticle-concanavalin A hybrid nanoflowers. Microchim Acta 186(2):57. https://doi.org/10.1007/s00604-018-3133-7
26. Ge J, Lei J, Zare RN (2012) Protein-inorganic hybrid nanoflowers. Nat Nanotechnol 7(7):428–432. https://doi.org/10.1038/nnano.2012.80
27. He Y, Ren Y, Guo B, Yang Y, Ji Y, Zhang D, Wang J, Wang Y, Wang H (2020) Development of a specific nanobody and its application in rapid and selective determination of Salmonella enteritidis in milk. Food Chem 310:125942. https://doi.org/10.1016/j.foodchem.2019.125942
28. Duan N, Shen M, Qi S, Wang W, Wu S, Wang Z (2020) A SERS aptasensor for simultaneous multiple pathogens detection using gold decorated PDMS substrate. Spectrochim Acta A Mol Biomol Spectrosc 230:118103. https://doi.org/10.1016/j.saa.2020.118103
29. Cai G, Zheng L, Liao M, Li Y, Wang M, Liu N, Lin J (2019) A microfluidic immunosensor for visual detection of foodborne bacteria using immunomagnetic separation, enzymatic catalysis and distance indication. Microchim Acta 186(12):757. https://doi.org/10.1007/s00604-019-3883-x
30. Bhandari D, Chen FC, Bridgman RC (2019) Detection of Salmonella typhimurium in romaine lettuce using a surface plasmon resonance biosensor. Biosensors (Basel) 9(3). https://doi.org/10.3390/bios9030094
31. Xiong J, Wang WX, Fu ZF (2017) Fluorimetric sandwich affinity assay for Staphylococcus aureus based on dual-peptide recognition on magnetic nanoparticles. Microchim Acta 184(10):4197–4202. https://doi.org/10.1007/s00604-017-2396-8
32. Zhu FJ, Zhao GY, Dou WC (2018) Electrochemical sandwich immunoassay for Escherichia coli O157:H7 based on the use of magnetic nanoparticles and graphene functionalized with electrocatalytically active Au@Pt core/shell nanoparticles.

Microchim Acta 185(10):455. https://doi.org/10.1007/s00604-018-2984-2

33. Li T, Yu LJ, Li MT, Li W (2006) A new approach to the standard addition method for the analysis of F, Al and K content in green tea. Microchim Acta 153(1–2):109–114. https://doi.org/10.1007/s00604-005-0454-0
34. Zhan Z, Li H, Liu J, Xie G, Xiao F, Wu X, Aguilar ZP, Xu H (2020) A competitive enzyme linked aptasensor with rolling circle amplification (ELARCA) assay for colorimetric detection of Listeria monocytogenes. Food Control 107(0956–7135):106806. https://doi.org/10.1016/j.foodcont.2019.106806
35. Mannoor MS, Zhang S, Link AJ, McAlpine MC (2010) Electrical detection of pathogenic bacteria via immobilized antimicrobial peptides. Proc Natl Acad Sci U S A 107(45):19207–19212. https://doi.org/10.1073/pnas.1008768107
36. Xie S, Ye J, Yuan Y, Chai Y, Yuan R (2015) A multifunctional hemin@metal-organic framework and its application to construct an electrochemical aptasensor for thrombin detection. Nanoscale 7(43):18232–18238. https://doi.org/10.1039/c5nr04532k
37. Pang B, Zhao C, Li L, Song X, Xu K, Wang J, Liu Y, Fu K, Bao H, Song D, Meng X, Qu X, Zhang Z, Li J (2018) Development of a low-cost paper-based ELISA method for rapid Escherichia coli O157:H7 detection. Anal Biochem 542:58–62. https://doi.org/10.1016/j.ab.2017.11.010